

# Nucleus Neural Network for Super Robust Learning

Jia Liu

School of Computer Science and Engineering, Nanjing University of Science and Technology  
Nanjing, 210094, China

omegalij@gmail.com

Maoguo Gong

School of Electronic Engineering, Xidian University  
Xi'an, 710071, China

gong@ieee.org

Haibo He

Department of Electrical, Computer, and Biomedical Engineering, University of Rhode Island  
Kingston, RI, 02881, USA

haibohe@uri.edu

April 9, 2019

## Abstract

Artificial neural networks which model the neurons and connecting architectures in brain have achieved great successes in many problems, especially those with deep layers. In this paper, we propose a nucleus neural network (NNN) and corresponding architecture and parameter learning methods. In a nucleus, there are no regular layers, i.e., a neuron may connect to all the neurons in the nucleus. This architecture gets rid of layer limitation and may lead to more powerful learning capability. It is crucial to determine the connections given numerous neurons. Based on the principle that more relevant input and output neuron pair deserves higher connecting density, we propose an architecture learning model for the nucleus. Moreover, we propose an improved learning method for learning connecting weights and biases with the optimized architecture. We find that this novel architecture is robust to irrelevant components in test data. So we define a super robust learning problem and test the proposed network with one case where the types of image

backgrounds in training and test sets are different. Experiments demonstrate that the proposed learner achieves significant improvement over traditional learners on the reconstructed data set.

## 1 Introduction

Mimicking the architecture and mechanism of nature creatures' learning for creating efficient and robust learners is one of the challenges in artificial intelligence research [1]. Artificial neural networks which model the mechanism of neurons and connecting architecture of them have excellent learning capability in many applications. Specially, neural networks with deep hierarchical layers have achieved many breakthroughs in machine learning, which leads to the great research interests in deep learning [13]. Deep learning is featured with deep hierarchical architectures trained by large scale datasets so that the learners are robust to various situations in real applications. Architecture including types

and scale of layers, depth, kernel size, and even presence of each connection, plays an important role in neural networks. Therefore, architecture learning has been a research interest for decades with various optimization methods [20, 29, 26, 2, 11, 21, 25, 17, 30, 10].

Concise architecture learning methods are based on the hierarchical architectures, i.e., multiple layers with no connections in the same layer. For example, NEAT algorithm used in [29] evolves the nodes, connections and weights for a network. In [30] and [10], the sparse connecting structure is focused and redundant connections are removed from a hierarchical compact network. With the increasing depth of neural networks, traditional hierarchical architecture may limit the learning capability. Therefore, there are some attempts trying to add additional skip connections [31, 15, 27, 28, 7] among which the most successful one is the residual network [7]. Residual network adds shortcut connections between input and output layers of a section of multilayer network to learn a residual function, i.e.,  $\mathcal{H}(x) - x$  with  $x$  and  $\mathcal{H}(x)$  respectively representing the input and output of the section of network. A very deep network can be constructed and more complicated models can be learned with these shortcut connections. This motivates the learning of more additional connections in architecture. For example, in [25], a complex architecture is evolved with involvement of not only multi-layer configurations but also skip connections. Nowadays, there are increasing interests in architecture learning based on network blocks or cells [17, 33, 16, 23]. A block or cell is a directed acyclic graph consisting of an ordered sequence of nodes [17]. The connections between them are optimized to achieved a better performance of classification or other tasks. Such architectures further relax the layer limitation and achieve larger learning capability. As a consequence, in this paper, we attempt to fully relax the architecture limitation and evolve the network architecture directly based on the neural nodes. A neural node is able to connect to any nodes and the connections are determined according to data and tasks. But since we focus on classification problem in this paper, the only limitation is that there are no feed-back connections. There is no regular layers in the new architecture and it is more like a nerve nucleus in brain. Thus we call it nucleus neural network (NNN). Fig. 1 exhibits the architectures learned by different architecture learning methods.

However, searching in such a large scale space is of

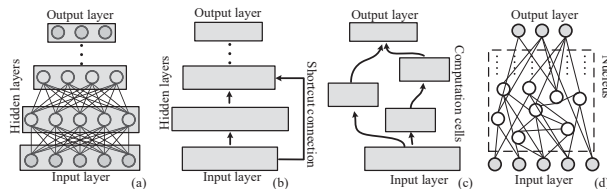


Figure 1: Architectures learned by different methods. (a) Multi-layer network (b) Multi-layer network with shortcut connections (c) Architecture learned based on neural network cells (d) Architecture of NNN

great difficulty. It is crucial to design an efficient objective function. Most of architecture learning methods search the optimal architecture based on task itself as the objective, for instance, test error for classification. But it is computationally demanding even though the searching space in them is not that large. For example, 1800 GPU days of reinforcement learning is required to search the optimal architecture in [33] and 3150 GPU days of evolution in [23]. There are also many methods proposed to speed up the learning process, such as weight sharing [4], Bayesian optimisation [12], and differentiable network architecture search [17]. However, most of them focus on reducing the searching space or increasing searching efficiency. In NNN, the optimizer should search in a binary space with over ten thousand dimensions which is much larger than that of most existing architecture learning problems. As a consequence, we propose a substitutable but more efficient objective function with respect to the architecture. We define a connecting density between a neuron and an input neuron. Then if an input neuron is more relevant to an output neuron according to the mutual information computed from the training data, the connecting density between them should be larger. The objective function is defined based on this principle via the modeling approach of products of experts (PoE) [8] in order to capture the distribution of observed data directly by the architecture without the involvement of weights and biases. This will greatly reduce the computational complexity of objective function. A binary particle swarm optimizer (BPSO) algorithm [6] is utilized to optimize the objective function. After the architecture is optimized, the connecting weights and biases are learned by a novel error driven probability model to well represent the input data.

After training, we find an interesting phenomenon of NNN. Since the architecture is evolved based on the input and output relevance, NNN gives high response to the data where patterns of irrelevant components are never seen by NNN during training. This means that NNN is robust to background changes when trained only by images with pure background in image classification. To highlight the superiority of NNN, we define a new learning problem which is significant but more difficult than traditional learning problems. NNN is able to deal with one case of this problem and we construct a new data set where the background types of training and test data are different. NNN achieves significant improvements in classification performance on this data set.

## 2 NNN's Architecture Learning

Fig. 1(d) shows the architecture of NNN. NNN fully relaxes the limitation in architecture and the connections are evolved based on neural nodes instead of layers or blocks. NNN is composed of input layer, output layer and a nucleus. In the nucleus, there are no regular layers and a neuron can connect to any neurons. But for time independent data, feedback connections are unallowed. We define a novel objective function for evolving the connections. In order to reduce the computational complexity, we directly model the connections without considering the connecting weights and biases. It is established based on the principle that higher relevance leads to higher connecting density so as to learn the relationship between input and output nodes. First the connecting density is defined.

### 2.1 Connecting Density

To evaluate the architecture, we should consider not only depth but also width of the information flow between an input and an output neurons. Therefore, we define a propagated connecting density with the initial density between an input neuron and itself being 1. Then the density  $\mathcal{D}_{ij}(\varphi)$  between a neuron  $i$  in the nucleus and an input neuron  $j$  can be computed as follows:

$$\mathcal{D}_{ij}(\varphi) = \frac{\sum_{k \in \Omega_i} \mathcal{D}_{kj}(\varphi)}{N_{\Omega_i}} \quad (1)$$

where  $\varphi$  denotes the architecture of the network which is a binary matrix indicating the connecting status between each pair of neurons with 1 denoting connected and 0 unconnected.  $\Omega_i$  denotes the set of lower neurons that directly connect to  $i$  and  $N_{\Omega_i}$  is the number of neurons in the set. It means the average connecting density from the lower neural nodes and can be simply read as the residue of input information. The connecting density starts from the input neurons, propagates through the connections, and finally that between input and output neurons is obtained. The connecting density represents a information path between an input and an output neurons. From Eq. (1), higher density means wider and shallower path with more processing nodes and less information degression. If the path is deeper, the information of this input neuron will be disturbed by information from other neurons. Therefore, the density will be lower. The information path should well adapt to the relevance between input and output neurons. Based on this principle, we then construct the model of each output neuron.

### 2.2 Modeling Single Output Neuron

Here we utilize the normalized pointwise mutual information (NPMI) [3] to represent the relevance between input and output neurons for each data. Suppose an input neuron  $j$  and an output neuron  $i$ , given a pair of input and output neurons' status  $\{x_j, y_i\}$  with input vector  $x$  and referenced output vector  $y$ , the NPMI between them  $\mathbb{N}(x_j; y_i)$  can be computed by:

$$\mathbb{N}(x_j; y_i) = \frac{\mathbb{I}(x_j; y_i)}{\mathbb{H}(x_j, y_i)} = \log \frac{P(x_j, y_i)}{P(x_j)P(y_i)} / \log \frac{1}{P(x_j, y_i)} \quad (2)$$

where  $\mathbb{I}$  denotes the pointwise mutual information (PMI) and  $\mathbb{H}$  denotes the self-information.  $P(\ )$  denotes the probability which is counted from the dataset. The NPMI normalizes PMI into an interval of  $[-1, 1]$  with  $-1$  denoting the two values will never occur together, 0 independence, and 1 complete co-occurrence. Because the probability of a negative valued  $\mathbb{N}(x_j; y_i)$  is very small and can be omitted, we define the relevance between  $x_j$  and  $y_i$  as  $\mathbb{R}(x_j, y_i) = \max(\mathbb{N}(x_j; y_i), 0)$  [5] to avoid unexpected overflow.

The connecting density should follow the relevance for a better information flow of input and output neurons.

Therefore, the possibility that an output neuron and its corresponding information path can well represent the input vector is measured by the cosine distance between relevance and connecting density:

$$p_i(x, y_i; \varphi) = \cos(\mathcal{D}_i(\varphi), \mathbf{R}(y_i)) \quad (3)$$

where  $\mathcal{D}_i(\varphi)$  and  $\mathbf{R}(y_i)$  respectively denotes the connecting density and relevance vectors with  $n$  dimensions, i.e.,  $\mathcal{D}_i(\varphi) = [\mathcal{D}_{i1}(\varphi), \mathcal{D}_{i2}(\varphi), \dots, \mathcal{D}_{in}(\varphi)]^T$  and  $\mathbf{R}(y_i) = [\mathbf{R}(x_1, y_i), \mathbf{R}(x_2, y_i), \dots, \mathbf{R}(x_n, y_i)]^T$  where  $n$  is the number of input neurons. For an architecture that best captures the relevance between an output neuron and input neurons, the possibility, i.e., cosine distance will be close to 1. While if there is no enough connecting density for transforming the information, the possibility will be close to 0.

### 2.3 Modeling the Whole Network

The whole network can be modeled by combining the models of output neurons. For better modeling the high-dimensional space of input data, in this paper, we combine the neurons by multiplying them together and renormalizing as in PoE. PoE has the advantage that they can produce much sharper distributions [8]. In NNN, the whole network model is formulated as follows:

$$p(x, y; \varphi) = \frac{\prod_i p_i(x, y_i; \varphi)}{\sum_{(\chi, \gamma)} \prod_i p_i(\chi, \gamma_i; \varphi)} \quad (4)$$

where  $(\chi, \gamma)$  denotes one of all the possible data in the whole data space which  $(x, y)$  belongs to. The denominator is the renormalization term used to guarantee that the probability sum over the whole data space is 1. The model follows PoE where simple models  $p_i(x, y_i; \varphi)$  are multiplied and renormalized to construct a complex model  $p(x, y; \varphi)$ . Optimizing this model means to increasing the representation capability of observed data while decreasing that of all the other data. Then the architecture  $\varphi$  will well capture the distribution of observed data.

However, optimizing this model is of great difficulty due to the unreachable fantasy data in the whole data space. In PoE, the model is optimized by using the gradient of a log-likelihood. Gibbs sampling is used to estimate the gradient expectation of the whole data space.

However, in this model, the decision variable is the architecture  $\varphi$  which is binary. Such a problem is suitable to be solved by evolutionary algorithms or population based methods [24, 18]. Therefore, we intend to optimize the architecture via a binary particle swarm optimization (BPSO) algorithm. A computable objective function is necessary to be derived.

### 2.4 Objective Function

Fortunately, the value of the denominator in Eq. (4) depends only on the architecture  $\varphi$ . Optimizing this model amounts to maximizing the numerator while minimizing the denominator. Therefore, the denominator can be replaced by a computable function with respect to  $\varphi$  and taken as a new term added to the numerator. Here we use the L2-norm of connecting density vector of each output neuron:

$$\rho(\varphi) = \sum_i \|\mathcal{D}_i(\varphi)\|_2 \quad (5)$$

The denominator in Eq. (4) aims to represent the whole data space by connecting density. Since the whole data space contains all the possible cases, connecting density controls the representation ability of the architecture for all the possible data. Therefore, minimizing  $\rho(\varphi)$  will decrease the denominator in Eq. (4).

Then the new objective function can be reconstructed by combining the two terms, i.e., numerator in Eq. (4) and Eq. (5):

$$\max J(\varphi) = \sum_{(x, y) \in \mathbf{D}} \prod_i p_i(x, y_i; \varphi) - \lambda \rho(\varphi) \quad (6)$$

where  $\mathbf{D}$  is the training set and  $\lambda$  is a user defined parameter that controls the importance of the two terms. In this objective function, the denominator in Eq. (4) is replaced by a simplified function but can achieve similar effectiveness to that of Eq. (4). Maximizing this function amounts to assigning more probability to the observed data (increasing numerator) while restraining the probability of all the other data (decreasing denominator). Then the architecture will capture the distribution of observed data and well represent the input and output relationship of the data in data set  $\mathbf{D}$ . Finally we utilize a BPSO algorithm to optimize the objective function.

## 2.5 Optimization via BPSO

In BPSO, we directly encode the individuals as  $\varphi$  and construct the population  $\Phi = \{\varphi^1, \varphi^2, \dots, \varphi^m\}$  where  $m$  is the number of individuals in the population. These individuals move according to a velocity which is induced by personal best solutions and global best solution:

$$v_g^i = v_{g-1}^i + c_1 \text{rand}(0, 1)(P_{best}^i - \varphi_g^i) + c_2 \text{rand}(0, 1)(G_{best} - \varphi_g^i) \quad (7)$$

where  $v_g^i$  denotes the velocity of the  $i$ -th individual in the  $g$ -th generation.  $P_{best}^i$  denotes the best solution searched by the  $i$ -th individual and  $G_{best}$  denotes the best solution searched by all the individuals in the population.  $\text{rand}(0, 1)$  is a random number in the range of  $[0, 1]$ .  $c_1$  and  $c_2$  are user defined parameters that controls the importance between global and local search. Then the probability for components in a new solution being 1 is computed by:

$$S_g^i = \frac{1}{1 + \exp(-v_g^i)} \quad (8)$$

where  $S_g^i$  is the probability matrix of the  $i$ -th individual and then the new solution of the  $i$ -th individual  $\varphi_{g+1}^i$  will be sampled from the possibility matrix. After all the individuals are updated, the best solutions including  $P_{best}$  and  $G_{best}$  will be updated. Then the process goes to the next generation. These steps will be repeated until the stop criteria is satisfied which is usually the maximum number of iterations. Finally we obtain an architecture that well represents the input and output relationship.

## 2.6 Toy Example of Learned Architecture

To better explain the whole story, we provide a toy example of the learned architecture from a simulated data set. The data set is constructed as a classification problem. There are 4 dimensions in the input data with the first 3 dimensions following the joint Gaussian distribution and the last dimension follows the uniform distribution. In the learning process, we set 10 neurons in the nucleus and Fig. 2 shows the learned architecture. It is intuitive that the first 3 dimensions contribute more to the classification, and therefore more connections are connected to them. They also directly connect to the output neurons. We set 10 neurons in the nucleus but after learning, there is 1

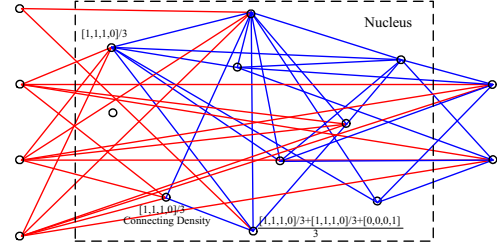


Figure 2: A toy example of learned architecture from a simulated data set. Red lines represents the connections from input neurons.

neuron unused. This means that 9 neurons are enough to represent the relationship between input and output neurons.

The computation of connecting density between some neurons and input neurons are also shown in Fig. 2. The initial connecting density of input neurons are 1. As shown in the figure, the connecting density between a neuron and input neurons is represented as a vector. Then they propagate through the whole network and  $\mathcal{D}_i(\varphi)$  for each output neuron is obtained.

## 3 NNN's Parameter Learning

After the architecture is learned, the network parameters, i.e., the weights on each connection and bias on each neuron, have also to be learned to achieve the function of classification or other tasks. Back-propagation is the common method that trains multi-layer neural networks. In multi-layer network, the errors can be back-propagated layer by layer and then the gradient of parameters can be obtained by the back-propagated errors. However, in NNN, different neurons have different depth. Even though the errors can also back-propagate from output layer, the different depth leads to different error decay. Then, the different error decay leads to uneven impact of reference output on input neurons. Therefore, some weights may not be well trained by directly using back-propagation.

### 3.1 NNN's Parameter Learning Model

In the parameter learning process, we should not only consider the errors in the output layer, but also consider the representation capability for input data. As a consequence, similar to RBM, we construct a probability model with the errors in the output layer as the energy:

$$p(x|y; \theta) = \frac{\exp(-E(x, y; \theta))}{\sum_{\chi} \exp(-E(\chi, y; \theta))} \quad (9)$$

where  $E(x, y; \theta)$  is the square error between output of the network  $f_{\theta}(x)$  and reference output  $y$ , i.e.,  $E(x; \theta) = \|y - f_{\theta}(x)\|_2^2$  with  $\theta$  being the network parameter set. Similar to the architecture model,  $\chi$  denotes all the possible data in the whole data space. This model denotes a parameterized probability density that captures the distribution of observed data given a reference output.

### 3.2 Optimization

This model can be solved via the gradient of log-likelihood:

$$\begin{aligned} \Delta\theta &= \frac{\partial \log p(x|y; \theta)}{\partial \theta} \\ &= \frac{\partial -E(x)}{\partial \theta} - \sum_{\chi} \frac{\exp(-E(\chi))}{\sum_{\chi} \exp(-E(\chi))} \frac{\partial -E(\chi)}{\partial \theta} \\ &= \frac{\partial -E(x)}{\partial \theta} - \mathbb{E}_{p(\chi|y; \theta)} \frac{\partial -E(\chi)}{\partial \theta} \end{aligned} \quad (10)$$

where  $\mathbb{E}$  denotes the expectation. The first term in Eq. (10) is easy to compute with the back-propagation algorithm. For the second term, we use the data  $\hat{x}$  sampled from the distribution  $p(x|y; \theta)$  to estimate the expectation of gradients. However, with the complex architecture, it is difficult and even impossible to compute the probability of each input neuron. Therefore, we propose to solve the problem in reverse.

The sampled data is more likely to locate in the high density region of the distribution. Therefore, we can drive a random sample to move to the high density region by gradient, i.e.,  $\Delta\hat{x} = \partial p(\hat{x}|y; \theta) / \partial \hat{x}$ . During the sampling process, the network parameter set  $\theta$  is fixed which leads to the dominator in Eq. (9) being a constant. Then the

updating gradient is computed as follows:

$$\Delta\hat{x} = \frac{\partial \exp(-E(\hat{x}))}{\partial \hat{x}} = \exp(-E(\hat{x})) \frac{\partial -E(\hat{x})}{\partial \hat{x}} \quad (11)$$

The gradient is then the error back-propagated from the output layer. The sampled data  $\hat{x}$  is then obtained by the gradient iteratively. This process will repeat several times to obtain several sampled data and estimate the expectation. After that, the gradient in Eq. (10) can be computed by using back-propagation for each term. The whole learning process is exhibited in Algorithm 1.

---

#### Algorithm 1 Parameter Learning Process of NNN

---

**Initialization:** initialize the connecting weights and biases randomly.

**Repeat:**

**Sampling:** update a randomly initialized  $\hat{x}$  according to the gradient in Eq. (11) for several times and obtain the sampled data  $\hat{x}$ .

**Estimating:** repeat the sampling several times and estimate the expected gradient  $\mathbb{E}_{p(\chi|y; \theta)} \frac{\partial -E(\chi)}{\partial \theta}$  by several sampled data  $\hat{x}$ , i.e.,  $\sum_{\hat{x}} \frac{\partial -E(\hat{x})}{\partial \theta}$

**Updating:** compute the gradient  $\frac{\partial -E(x)}{\partial \theta}$  with the observed data  $x$  and obtain the updating gradient of  $\theta$  in Eq. (10).

**Stop Criterion:** stop the iteration process when the training error is lower than a threshold or the number of iterations exceeds maximum value.

---

This new model and learning process can relieve the uneven impact of output neurons. The updating gradient is the difference between gradients of observed data and sampled data. For a deep path, there is more error decay from the output layer. Then the components of deep paths in a sampled data is more random. Thus the gradient difference between observed data and sampled data will be larger. While for a shallow path, the gradient difference will be smaller. Then the uneven impact will be offset by the uneven difference. By the probability model, the learned network parameter set can minimize the training loss and meanwhile well capture the distribution of primary components. Due to the relevance affected architecture, the information loss from each input component to output components is different. As a consequence, some irrelevant components can be eliminated by the network.

### 3.3 Toy Example of Parameter Learning

Similarly, we provide a toy example to explain the observed distribution and sampled distribution by the network. We train the network architecture and parameters by a simulated data set. There are 3 dimensions in each data. The first two dimensions follow the joint Gaussian distribution and the last dimension is a constant. The distribution of the simulated data is shown by the blue points in Fig. 3. There are two classes and different classes follow Gaussian distribution with different parameters.

In Fig. 3, the distribution assigned by the network is shown by the red points. With the randomly initialized network, the sampled data  $\hat{x}$  are randomly distributed. During the learning process, the network begins to capture the distribution of observed data. Therefore, the sampled data begin to follow the observed distribution. After learning, the learned network can well capture the distribution of the first two dimensions in the observed data. Because the first two dimensions play important roles in decision, the network assigns more connecting density for them. Then the network can learn to follow the distribution of them by connecting weights and biases. The last dimension has no contributions to classification and thus that of the sampled data is approximately randomly distributed after learning.

This novel phenomenon demonstrates that NNN infers unseen cases. In other words, NNN is robust to irrelevant components, i.e., the background. The sampled distribution represents the energy driven response of the network to different data. That means, the samples at the higher density region have lower energy, i.e., output difference from reference. Therefore, NNN assigns high response to the data indicated by red points in Fig. 3. In other words, all the data indicated by red points can achieve low classification error although the distribution in the last dimension is much different from that of training data. As a consequence, in this paper, we define a new learning problem which is significant but challenging, i.e., super robust learning and use one case to test the proposed NNN.

## 4 Super Robust Learning and Experiments

### 4.1 Super Robust Learning

In supervised learning, it is usually supposed that the training data set and test data set are independent and identically distributed. Given a set of labeled data  $\{x^i, y^i\}_{i=1}^N$  with  $N$  being the number of data, many traditional learners try to estimate the conditional distribution  $P(x|y)$  (Bayesian learning) or learn to maximize the parameterized conditional distribution  $p(y^i|x^i; \theta)$  (discriminative models). Then given a test data  $\hat{x}$  in real applications,  $p(\hat{y}|\hat{x})$  is estimated and the correct label is determined. If there is bias between distributions of  $x$  and  $\hat{x}$ ,  $p(\hat{y}|\hat{x})$  will not be correctly estimated. Therefore, for robust learning in real applications, a large scale labeled data set covering most cases is required and meanwhile a deep architecture that could model the complicated distribution is also necessary. However, constructing such a data set is a hard work. As a consequence, sample selection bias in transfer learning [22] poses this problem and solves it by transferring the knowledge from labeled data in source domain to unlabeled data in target domain. But transfer learning methods suppose that source domain and target domain are not independent. They estimate the bias with the help of unlabeled data. In this paper, we pose a more difficult problem.

We define a super robust learning problem as a learning problem where training data set and test data set are independent but follow different distributions partly. For instance, a learner which is trained by limited images should be robust to background changes, different view angles, or different types of sensors. In this problem, a learner is expected to adapt to various cases in real applications when trained by labeled data of limited cases. During the training process, test data is not available to estimate the bias. Some specially designed learners may be tolerant to slight bias. For example, the widely used convolutional neural networks (CNN) [14] are robust to shift variance in test images due to the use of pooling layers. CoordConv in [19] addresses intriguing failing of CNN in coordinate transform problem and solves the problem with perfect generalization. Transfer learning [22] can deal with various biases based on the dependence between labeled and

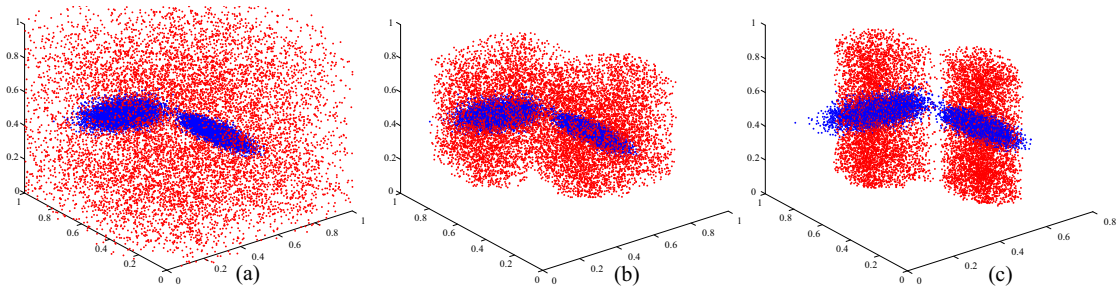


Figure 3: Distribution of observed data and sampled data in different learning stages. The blue points denote the observed data and red ones are sampled data. (a) Sampled distribution by randomly initialized network. (b) Sampled distribution by the network during the learning process. (c) Sampled distribution by the network after training.

unlabeled data. However, without any prior information about the test data, transfer learning is impossible to be implemented.

Due to the consideration of relevance between input and output nodes, NNN is robust to irrelevant components, i.e., background. Suppose one component  $x_i$  is the background component, the independence between  $x_i$  and  $y$  also leads to the independence between input and output nodes. Then for a test data  $\hat{x}$ ,  $p(\hat{y}|\hat{x}_i) = p(\hat{y})$ . This means that whatever the  $\hat{x}_i$  is, the output will not be influenced. Therefore, in this paper, we consider one case of super robust learning problem, i.e., different backgrounds and construct a new data set based on the widely used MNIST digit data set.

## 4.2 Data Set

A smart learner should recognize the digits under different backgrounds when taught only on the blackboard. Therefore, we train the learners by the training set in the MNIST data set and apply the trained learner to digits with various backgrounds. Fig. 4 shows some images in the training set and test set. MNIST data set is a collection of handwritten digits (0-9) which is used to train and test classifiers for handwritten digit recognition. However, in practice, there are also digits on various backgrounds. Then some derivatives of MNIST data set are created, including MNIST digits with random image background (bg-img) and random noise background (bg-rand) [32]. In super robust learning, the classifiers should recognize such digits when trained by pure digits.

In the experiments, 60000 training digits in the MNIST data set are used to train the classifiers. Then 50000 digits with bg-img and 50000 digits with bg-rand are used to test the classifiers. It deserves to be noted that training and test processes are independent, i.e., the digits in test set have no influence on the training process. To my knowledge, few methods could perfectly solve this problem. We set the number of neurons in the nucleus to be 200 and  $\lambda = 1$ . We compare the proposed NNN with architectures of DBN and CNN. We set the scale of DBN as “784-500-300-10” [9] and CNN as LeNet in [14]. All the three architectures are trained by both back-propagation (BP) and the proposed error driven probability model (EDPM). The experimental results are evaluated by receiver operating characteristic (ROC) curve, precision-recall (PR) curve, area under ROC curve (AUC), area under PR curve (AP), and the classification accuracy (CA).

## 4.3 Experimental Results

First we demonstrate the learning capability of NNN on traditional classification problem where the digits in training and test set follow the same distribution. After trained by the training set in MNIST data set, the classifiers are used to classify the digits in the test set. The ROC and PR curves of each classifier is shown in Fig. 5. It can be found that NNN cannot outperform traditional classifiers in this problem. The values of AUC, AP, and CA are listed in Table 4.3. CNN achieves the best performance from the classification accuracy due to its special architecture. Although NNN achieves the lowest classification accuracy,

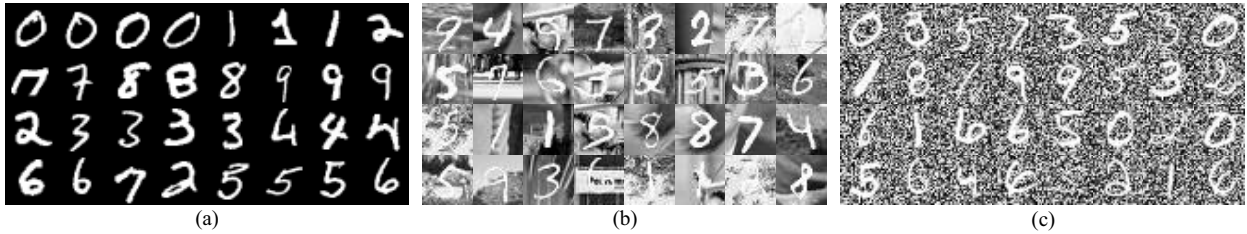


Figure 4: Some images in training and test data sets. (a) Training set with pure background. (b) Test set with random image patches as background. (c) Test set with random noise as background.

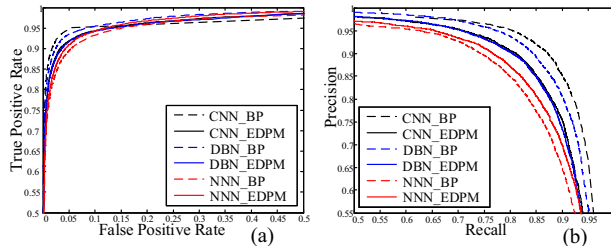


Figure 5: ROC and PR curves of the test result on digits in MNIST test set. (a) ROC curves (b) PR curves

Arc.	DBN		CNN		NNN	
Par.	BP	EDPM	BP	EDPM	BP	EDPM
AUC	.9968	.9888	.9864	.9898	.9846	.9921
AP	.9941	.9896	.3561	.9921	.8734	.9814
CA(%)	98.97	98.74	99.14	98.73	98.69	98.86

Table 1: AUC, AP, and CA values of the test result on digits in MNIST test set. Arc. denotes architecture and Par. denotes parameter learning method.

the accuracy is close to that of DBN. It deserves to be noted that there are only 200 neurons in the nucleus and 146686 connections in the whole network after training. In DBN, there are 800 hidden units and 545000 connections and much more in CNN. Therefore, NNN achieves equivalent performance to that of DBN with less processing units and parameters.

The superiority of NNN is its robustness to irrelevant components in input data, such as background in images. Therefore, we continue to use the trained classifiers to classify the digits with various backgrounds.

The ROC and PR curves of results on the two test sets, i.e., MNIST digits with bg-img and bg-rand, are shown in Fig. 6 and Fig. 7 respectively. For the digits with bg-img, the curves of NNN cover most of other curves and for the digits with bg-rand, the curves of NNN cover all the other curves. Traditional architecture and learning methods are ineffective to deal with problems where the distributions of training set and test set are different. Because traditional architectures are composed of hierarchical layers, input neurons have approximately equal impact on the output neurons from architecture. During the back-propagation process, the output errors will not influence the weights of background pixels a lot due to the weak contribution of them. Therefore, back-propagation could not weaken the influence of background changes on output. Then when images in training and test set are with different backgrounds, the classification results will be different a lot. The architecture of NNN fully considers the relationship between input and output neurons by different depth and number of connections. Thus the background neurons will be directed into deeper and narrower paths because they have much less impact on the output neurons. Therefore, NNN is more robust and greatly outperforms the traditional architectures.

Then the AUC, AP, and AC values of the two test sets are listed in Table 4.3 and Table 4.3 respectively. It can be found that CNN achieves worst performance in this problem. Because in CNN, the parameters in local convolutional kernels are shared, the background and foreground use the same kernels. Therefore, the influence of background neurons on the output neurons will be larger compared with the architectures of DBN and NNN. The proposed parameter learning method decreases the performance of hierarchical architectures because the model

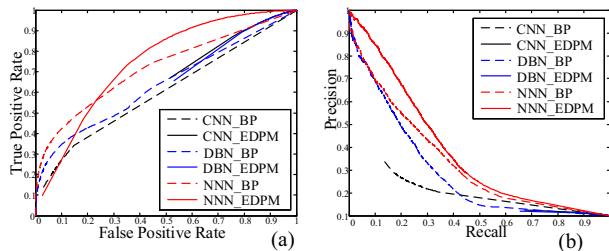


Figure 6: ROC and PR curves of the test result on digits with image background. (a) ROC curves (b) PR curves

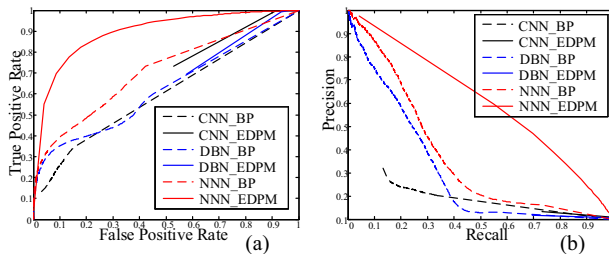


Figure 7: ROC and PR curves of the test result on digits with noise background. (a) ROC curves (b) PR curves

increases the energy, i.e., the training error of other data and decreases the energy of observed data. This means that with a distribution that is even a little different from distribution of training data, the output will be much different. Thus with different background in the test set, the performance decays a lot. However, in NNN, the background are restrained by the architecture, thus the model will specially focus on the foreground. Therefore, NNN greatly improves the performance in this super robust learning problem. The digits with bg-img are more difficult to recognize because the background greatly disturb the digits as shown in Fig. 4. Although NNN cannot achieve equivalent performance compared with traditional classifiers trained by images with the same kind of background as shown in [32], it outperforms traditional classifiers greatly when the backgrounds of training and test sets are different. The robust learning and inference capability of NNN is larger than that of traditional learning architectures in this data set.

Arc.	DBN		CNN		NNN	
Par.	BP	EDPM	BP	EDPM	BP	EDPM
AUC	.6395	.4005	.6002	.4139	.7205	.7434
AP	.2860	.0389	.1514	.0379	.3300	.3776
CA(%)	29.71	10.28	24.24	13.14	37.18	57.33

Table 2: AUC, AP, and CA values of the test result on digits with image background.

Arc.	DBN		CNN		NNN	
Par.	BP	EDPM	BP	EDPM	BP	EDPM
AUC	.6230	.3671	.5981	.4183	.7082	.8926
AP	.3020	.0340	.1478	.0323	.3658	.5685
CA(%)	30.66	9.55	22.18	15.62	32.84	67.00

Table 3: AUC, AP, and CA values of the test result on digits with noise background.

## 5 Conclusions and Future Work

This paper attempts a new neural network architecture which is called nucleus neural network (NNN). NNN mimics nuclei in brain where there is no regular layers so as to relax the limitation of layers. To evaluate the architectures efficiently, the architecture is modeled based on the principle that higher relevance of a pair of input and output neurons deserves a shorter and wider path. With the optimized architecture, the connecting weights and biases are learned by establishing a probability model in order to well represent the input data. We find that this novel architecture is robust to irrelevant components in data. This means that NNN works when the background of test data is different from that of training data. Therefore, we define the super robust learning problem and test the proposed NNN by a reconstructed data set. From the experiments, NNN is superior over traditional deep learners on this data set.

However, there are still many defects including the low architecture and parameter learning efficiency and unsatisfactory classification accuracy. The future work includes but is not limited to: (1) We will further improve the learning model and optimization methods in order to achieve higher accuracy in classification of objects on different backgrounds. (2) NNN is promising for super robust problems, therefore we will explore other super

robust learning problems via NNN by designing different architecture learning models. For example, for different imaging sensors, the architecture should be modeled based on the structure information of input data and for different view angles, the robustness to local variance should be used to guide the architecture learning. (3) There are no feedback connections for time independent data in this paper. We will also attempt feedback connections for time series data. (4) Inspired from hierarchical architecture of human brain, we will stack NNN into multiple nuclei for larger learning capability.

## References

- [1] I. Arel, D. C. Rose, T. P. Karnowski, et al. Deep machine learning—a new frontier in artificial intelligence research. *IEEE computational intelligence magazine*, 5(4):13–18, 2010.
- [2] J. Bergstra and Y. Bengio. Random search for hyperparameter optimization. *Journal of Machine Learning Research*, 13(1):281–305, 2012.
- [3] G. Bouma. Normalized (pointwise) mutual information in collocation extraction. *Proceedings of GSCL*, pages 31–40, 2009.
- [4] H. Cai, T. Chen, W. Zhang, Y. Yu, and J. Wang. Efficient architecture search by network transformation. In *Proceedings of AAAI Conference on Artificial Intelligence*, 2018.
- [5] K. W. Church and P. Hanks. Word association norms, mutual information, and lexicography. *Comput. Linguist.*, 16(1):22–29, Mar. 1990.
- [6] A. A. Esmin, R. A. Coelho, and S. Matwin. A review on particle swarm optimization algorithm and its variants to clustering high-dimensional data. *Artificial Intelligence Review*, 44(1):23–45, 2015.
- [7] K. He, X. Zhang, S. Ren, and J. Sun. Deep residual learning for image recognition. In *Proceedings of the IEEE conference on computer vision and pattern recognition*, pages 770–778, 2016.
- [8] G. E. Hinton. Training products of experts by minimizing contrastive divergence. *Neural computation*, 14(8):1771–1800, 2002.
- [9] G. E. Hinton, S. Osindero, and Y.-W. Teh. A fast learning algorithm for deep belief nets. *Neural computation*, 18(7):1527–1554, 2006.
- [10] L. Jia, M. Gong, Q. Miao, X. Wang, and L. Hao. Structure learning for deep neural networks based on multiobjective optimization. *IEEE Trans Neural Netw Learn Syst*, 29(6):2450–2463, 2018.
- [11] R. Jozefowicz, W. Zaremba, and I. Sutskever. An empirical exploration of recurrent network architectures. In *Proceedings of the International Conference on Machine Learning*, pages 2342–2350, 2015.
- [12] K. Kandasamy, W. Neiswanger, J. Schneider, B. Poczos, and E. Xing. Neural architecture search with bayesian optimisation and optimal transport. *arXiv preprint arxiv:1802.07191*, 2018.
- [13] Y. LeCun, Y. Bengio, and G. Hinton. Deep learning. *nature*, 521(7553):436, 2015.
- [14] Y. LeCun, L. Bottou, Y. Bengio, and P. Haffner. Gradient-based learning applied to document recognition. *Proceedings of the IEEE*, 86(11):2278–2324, 1998.
- [15] C.-Y. Lee, S. Xie, P. Gallagher, Z. Zhang, and Z. Tu. Deeply-supervised nets. In *Artificial Intelligence and Statistics*, pages 562–570, 2015.
- [16] C. Liu, B. Zoph, M. Neumann, J. Shlens, W. Hua, L. J. Li, L. Fei-Fei, A. Yuille, J. Huang, and K. Murphy. Progressive neural architecture search. *arXiv preprint arxiv:1712.00559*, 2017.
- [17] H. Liu, K. Simonyan, and Y. Yang. DARTS: differentiable architecture search. *arXiv preprint arxiv:1806.09055*, 2018.
- [18] J. Liu, M. Gong, Q. Miao, X. Wang, and H. Li. Structure learning for deep neural networks based on multiobjective optimization. *IEEE transactions on neural networks and learning systems*, 29(6):2450–2463, 2018.
- [19] R. Liu, J. Lehman, P. Molino, F. P. Such, E. Frank, A. Sergeev, and J. Yosinski. An intriguing failing of convolutional neural networks and the coordconv solution. *arXiv preprint arxiv:1807.03247*, 2018.
- [20] G. F. Miller, P. M. Todd, and S. U. Hegde. Designing neural networks using genetic algorithms. In *Proceedings of the International Conference on Genetic Algorithms*, pages 379–384, 1989.
- [21] G. Morse and K. O. Stanley. Simple evolutionary optimization can rival stochastic gradient descent in neural networks. In *Proceedings of Genetic and Evolutionary Computation Conference*, pages 477–484, 2016.
- [22] S. J. Pan and Q. Yang. A survey on transfer learning. *IEEE Transactions on Knowledge and Data Engineering*, 22(10):1345–1359, 2010.
- [23] E. Real, A. Aggarwal, Y. Huang, and Q. V. Le. Regularized evolution for image classifier architecture search. *arXiv preprint arxiv:1802.01548*, 2018.
- [24] E. Real, S. Moore, A. Selle, S. Saxena, Y. L. Suematsu, J. Tan, Q. Le, and A. Kurakin. Large-scale evolution of

- image classifiers. In *Proceedings of the International Conference on Machine Learning*, 2017.
- [25] E. Real, S. Moore, A. Selle, S. Saxena, Y. L. Suematsu, J. Tan, Q. V. Le, and A. Kurakin. Large-scale evolution of image classifiers. In *Proceedings of the International Conference on Machine Learning*, pages 2902–2911, 2017.
- [26] T. Spahl and J. Brosnihan. Evolving memory cell structures for sequence learning. In *Proceedings of the International Conference on Artificial Neural Networks*, pages 755–764, 2009.
- [27] R. K. Srivastava, K. Greff, and J. Schmidhuber. Highway networks. *arXiv preprint arXiv:1505.00387*, 2015.
- [28] R. K. Srivastava, K. Greff, and J. Schmidhuber. Training very deep networks. In *Advances in neural information processing systems*, pages 2377–2385, 2015.
- [29] K. O. Stanley and R. Miikkulainen. Evolving neural networks through augmenting topologies. *Evolutionary Computation*, 10(2):99–127, 2002.
- [30] Y. Sun, X. Wang, and X. Tang. Sparsifying neural network connections for face recognition. In *Proceedings of IEEE Conference on Computer Vision and Pattern Recognition*, pages 4856–4864, 2016.
- [31] C. Szegedy, W. Liu, Y. Jia, P. Sermanet, S. Reed, D. Anguelov, D. Erhan, V. Vanhoucke, and A. Rabinovich. Going deeper with convolutions. In *Proceedings of the IEEE conference on computer vision and pattern recognition*, pages 1–9, 2015.
- [32] P. Vincent, H. Larochelle, I. Lajoie, Y. Bengio, and P.-A. Manzagol. Stacked denoising autoencoders: Learning useful representations in a deep network with a local denoising criterion. *Journal of machine learning research*, 11(Dec):3371–3408, 2010.
- [33] B. Zoph, V. Vasudevan, J. Shlens, and Q. V. Le. Learning transferable architectures for scalable image recognition. *arXiv preprint arxiv:1707.07012*, 2017.